DEVELOPMENTAL DYNAMICS 240:1365–1372, 2011

RESEARCH ARTICLE

Axonal Regeneration Proceeds Through Specific Axonal Fusion in Transected *C. elegans* Neurons

Brent Neumann,[1] Ken C. Q. Nguyen,[2] David H. Hall,[2] Adela Ben-Yakar,[3] and Massimo A. Hilliard[1]*

Functional neuronal recovery following injury arises when severed axons reconnect with their targets. In *Caenorhabditis elegans* following laser-induced axotomy, the axon still attached to the cell body is able to regrow and reconnect with its separated distal fragment. Here we show that reconnection of separated axon fragments during regeneration of *C. elegans* mechanosensory neurons occurs through a mechanism of axonal fusion, which prevents Wallerian degeneration of the distal fragment. Through electron microscopy analysis and imaging with the photoconvertible fluorescent protein Kaede, we show that the fusion process re-establishes membrane continuity and repristinates anterograde and retrograde cytoplasmic diffusion. We also provide evidence that axonal fusion occurs with a remarkable level of accuracy, with the proximal re-growing axon recognizing its own separated distal fragment. Thus, efficient axonal regeneration can occur by selective reconnection and fusion of separated axonal fragments beyond an injury site, with restoration of the damaged neuronal tract. *Developmental Dynamics 240:1365–1372, 2011.* © 2011 Wiley-Liss, Inc.

Key words: axonal fusion; axonal regeneration; *C. elegans*; axonal degeneration

Accepted 11 February 2011

INTRODUCTION

For an axon to regenerate after injury, the affected neuron must transform its damaged proximal stump into a regrowing axon with a growth cone, which then must extend past the injury site and re-establish connection with its original target tissues. Growth cone formation and axonal extension are regulated by both the intrinsic regenerative growth capacity of the adult neuron, as well as the extrinsic, often inhibitory, microenvironment of the developed organism (Harel and Strittmatter, 2006; Yiu and He, 2006; Hilliard, 2009). Calcium and cAMP levels, as well as the DLK-1 mitogen-activated protein kinase-signaling pathway and genes of the Krüppel-like transcription factor family, have been shown to be essential intrinsic factors for growth cone initiation and extension (Neumann and Woolf, 1999; Spira et al., 2001; Neumann et al., 2002; Hammarlund et al., 2009; Moore et al., 2009; Ghosh-Roy et al., 2010). A crucial inhibitory role for the regenerating axons was found for molecules such as Nogo, myelin-associated glycoprotein and oligodendrocyte myelin glycoprotein, and their receptors Nogo receptor, P75, TROY, and LINGO (Harel and Strittmatter, 2006; Yiu and He, 2006). Furthermore, developmental axonal guidance molecules such as UNC-6/Netrin, Slit, Ephrin B3, and Semaphorin 4D, have also been shown to affect regenerative axonal outgrowth and guidance (Pasterkamp et al., 2001; Benson et al., 2005; Wu et al., 2007; Gabel et al., 2008; Low et al., 2008). However, what happens to an axon beyond the injury site and how target re-innervation occurs, remains poorly understood. In different models proposed, target reconnection might occur through precise regrowth of the axon from the injury site toward its target following

Additional Supporting Information may be found in the online version of this article.

[1]Queensland Brain Institute, The University of Queensland, Brisbane, Australia
[2]Albert Einstein College of Medicine, Department of Neuroscience, Bronx, New York
[3]University of Texas at Austin, Department of Mechanical Engineering, Austin, Texas

Grant sponsor: NIH; Grant number: R01-NS060129; Grant sponsor: NHMRC; Grant number: 631634 and 569500.

***Correspondence to: Massimo A. Hilliard, Queensland Brain Institute, The University of Queensland, Brisbane, QLD 4072, Australia. E-mail: m.hilliard@uq.edu.au**

DOI 10.1002/dvdy.22606
Published online 17 March 2011 in Wiley Online Library (wileyonlinelibrary.com).

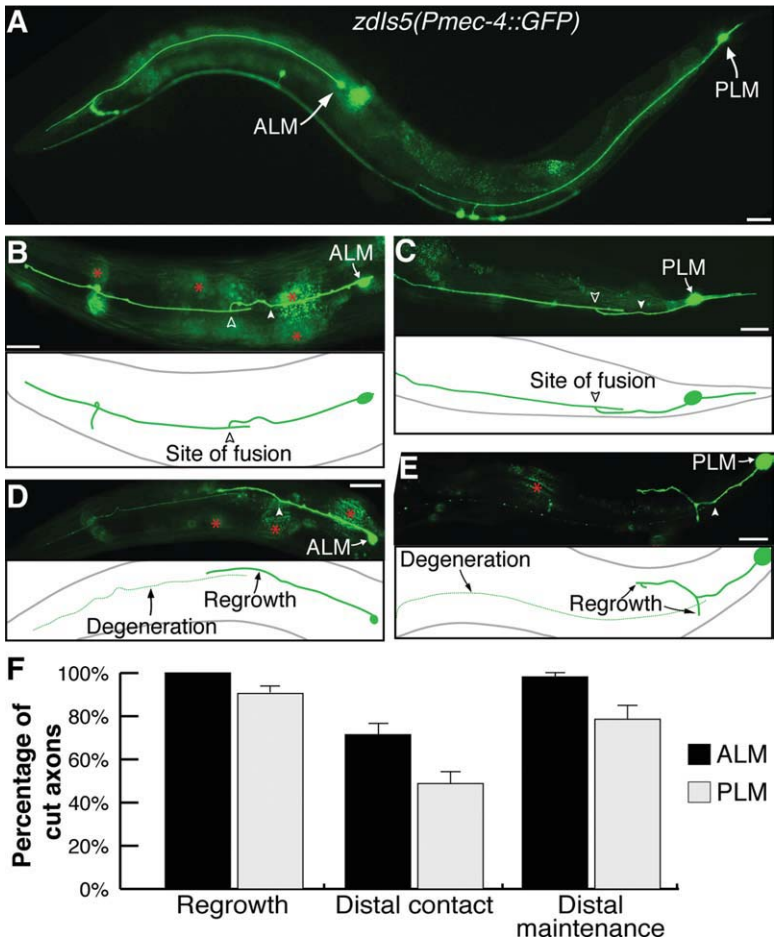

Fig. 1.

the original axonal path, or along an ectopic path, or through sprouting from an axonal region far from the injury site along an ectopic path (Harel and Strittmatter, 2006; Hilliard, 2009). Axonal fusion is an alternative form of axonal reconnection, whereby regenerating axons can bridge the site of damage and re-establish connection with their separated axonal fragments. This fusion process has been described in crayfish, earthworm, and leech (Hoy et al., 1967; Birse and Bittner, 1976; Deriemer et al., 1983; Macagno et al., 1985), although the cellular and molecular mechanisms regulating this process remain unknown. The development of laser-based surgery to transect individual axons in *C. elegans* (Yanik et al., 2004), has enabled this organism to become a crucial genetic model system to study axonal regeneration at the cellular and molecular level (Ghosh-Roy and Chisholm, 2010). Different *C. elegans* neurons have been widely reported to undergo robust regeneration following axotomy (Yanik et al., 2004, 2006; Wu et al., 2007; Gabel et al., 2008), and recent evidence suggests that axonal regeneration in *C. elegans* deficient in the cAMP phosphodiesterase gene (*pde-4*) may occur through axonal fusion (Ghosh-Roy et al., 2010). A fusion process also

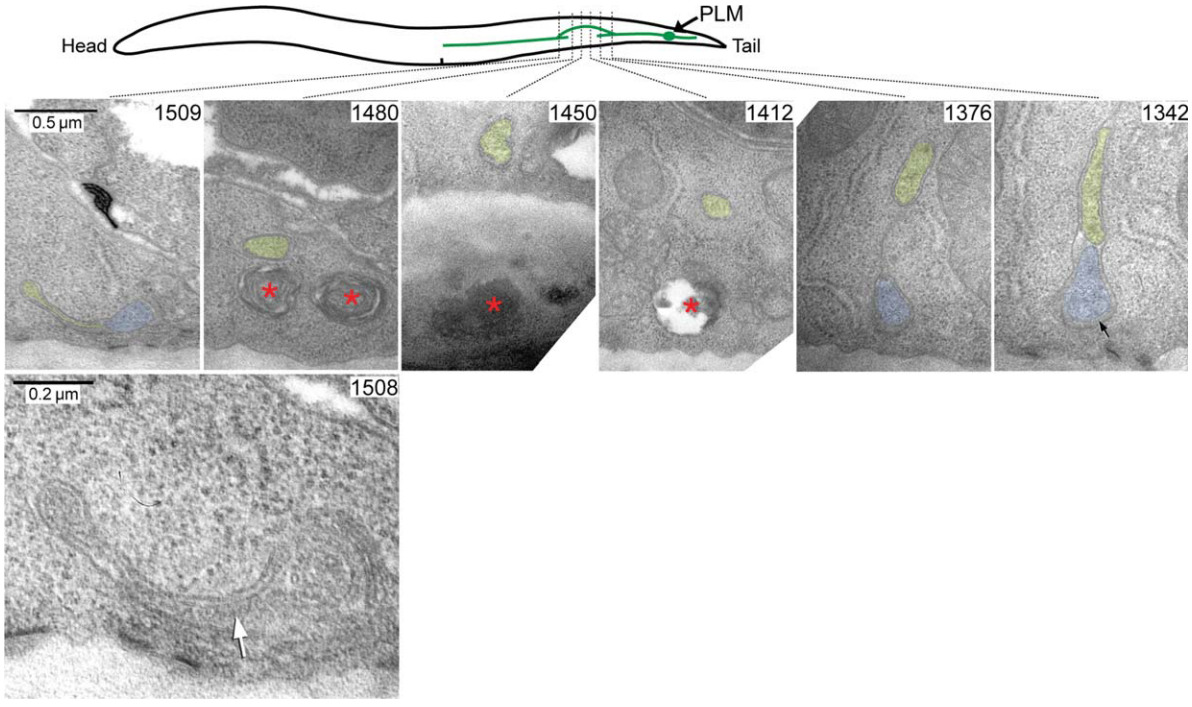

Fig. 2.

regulates pruning of excessive dendritic branches in the PVD neuron (Oren-Suissa et al., 2010).

Here, we conclusively demonstrate that following laser-induced axonal transection, the *C. elegans* mechanosensory neurons ALM and PLM undergo specific axonal fusion as a regenerative mechanism. We find axonal fusion to be critical for survival of the separated axonal fragment. We show that upon fusion, membrane continuity of the axonal tract is reconstituted, and that both anterograde and retrograde cytoplasmic diffusion is restored. Furthermore, we present evidence for a high level of specific recognition regulating fusion between the separated proximal and distal axonal fragments, suggesting the presence of error-checking or cross-talk to ensure accuracy of the repair mechanism.

RESULTS

The axons of the ALM and PLM mechanosensory neurons extend in an anterior direction from their cell bodies on both sides of the animal; ALM (left and right) in the anterior half and PLM (left and right) in the posterior half of the animal mediate detection of light mechanical stimuli applied to the head and tail regions, respectively (Bounoutas and Chalfie, 2007). The cell bodies and neurites of these neurons were visualized using green fluorescent protein (GFP) driven by the *mec-4* promoter (*Pmec-4::GFP*) (Fig. 1A). Following UV-laser axotomy, both neurons underwent extensive regrowth in over 90% of cases (Yanik et al., 2006) (Fig. 1B–F), as characterized by the formation of a growth cone at the tip of the proximal axon that on average extended 50–100 μm (Wu et al., 2007). Such regrowth frequently (71% for ALM; 48% for PLM) resulted in the proximal axon making contact with its separated distal fragment (Fig. 1B,C,F), an event that was essential for the survival of the separated fragment and for the restoration of the axonal structure (Fig. 1F). In the absence of proximal-distal axon reconnection, the distal process invariably underwent Wallerian degeneration, as evidenced by axonal beading, fragmentation, and ultimately disappearance of the distal axonal fragment (Fig. 1D,E). In a minority of cases (2% ALM; 21% PLM), reconnection between the separated axonal fragments was detected by visual analysis but degeneration of the distal fragment still progressed (Fig. 1F), indicating that either a successful contact was not established or that it had occurred too late to prevent degeneration from progressing.

To establish whether reconnection of the regrowing axon with its distal fragment was indeed a fusion of the two membranes, we performed transmission electron microscopy (TEM) analysis of serial sections taken from a wild-type animal 24 hr post-axotomy. As shown in Figure 2, PLM regrowth proceeded through extension of a branch from the proximal axon (Fig. 2, sections 1342, 1376) that circumvented the injury site (Fig. 2, sections 1412–1480) and reconnected with the distal fragment (Fig. 2, sections 1508, 1509). We found continuation of the plasma membrane between the regrowing axon and its distal fragment (Fig. 2, section 1508), demonstrating that the proximal-distal reconnection occurs through a fusion of the axonal membranes.

We then asked if this membrane fusion was sufficient for the re-establishment of cytoplasmic continuity. To address this, we analyzed both anterograde and retrograde cytoplasmic diffusion across the injury site using the Kaede protein. Kaede is a large tetrameric green fluorescent protein that can be irreversibly converted to fluoresce red (Ando et al., 2002), and that is too large to pass across gap junctions (Simpson et al., 1977; Loewenstein, 1981; see Supp. Fig. S1, which is available online). We generated a transgenic strain in which the Kaede coding sequence was driven by the *mec-4* promoter (*Pmec-4::Kaede*), and thereby expressed specifically within the mechanosensory neurons. First, to study anterograde cytoplasmic diffusion, we performed laser axotomies on ALM and PLM neurons expressing Kaede and irradiated the cell body and a short section of the attached process to convert Kaede from green to red specifically within this region. In the absence of proximal-distal reconnection, the converted, red form of the protein did not diffuse into the distal axon (Supp. Fig. S2A,C), indicating that cytoplasmic movement had been disrupted and that the axon had been completely transected. Twenty-four hours post-axotomy when proximal-distal reconnection had occurred, Kaede converted in the cell body was observed traversing the injury site and within the distal axonal segment (Fig. 3A,C; Supp. Fig. S2D; quantified in Supp. Fig. S2B,E), showing that anterograde diffusion had been re-established. Second, to analyze retrograde diffusion, we again performed axotomies on ALM and PLM, but converted Kaede in the distal axon and visualized movement of the red protein towards the cell body.

Fig. 1. Axonal regeneration in the *C. elegans* mechanosensory neurons. **A**: A wild-type *zdIs5*(*Pmec-4::GFP*) animal, illustrating the ALM and PLM mechanosensory neurons. Anterior is left and ventral is down in these and all other images. Reconnection between proximal and distal segments in ALM (**B**) and PLM (**C**), 24 hr post-axotomy. **D,E**: Degeneration of the distal axon occurs in the absence of reconnection. Filled arrowheads point to site of axotomy; open arrowheads show fusion site; asterisks highlight intestinal auto-fluorescence; scale bars = 25 μm. **F**: Quantification of regenerative phenotypes, with regrowth defined as sprouting from proximal end, distal contact representing the proportion of regrowing axons that made proximal-distal contact, and distal maintenance showing the percentage of reconnecting neurons that preserved the distal axon segment. Error bars: standard error of proportion; n values: 77 and 95 for ALM and PLM, respectively.

Fig. 2. Analysis of axonal reconnection with transmission electron microscopy. Serial thin sections of a wild-type animal 24 hr post-axotomy are shown, along with a scheme to demonstrate how the PLM axon regrew around the laser damage zone. High-magnification micrographs show the original axon (blue) and the new process (yellow) as it branched off from the original axon (section 1342), travelled inwards from the body wall (section 1376), traversed the damage site (section 1412–1480), and then fused as a very thin process (yellow) to the distal axon segment (blue) at section 1509. The fusion site is shown at higher power in section 1508, where the white arrow indicates the fusion zone. Local membrane whorls and voids (red asterisks) caused by collateral laser damage in the hypodermis can be seen in sections 1412, 1450, and 1480. Extracellular space below the PLM axon in section 1342 is swollen by mantle protein (black arrow), a characteristic feature of the mechanosensory neurons. Scale bars = 0.5 and 0.2 μm in sections 1509 and 1508, respectively.

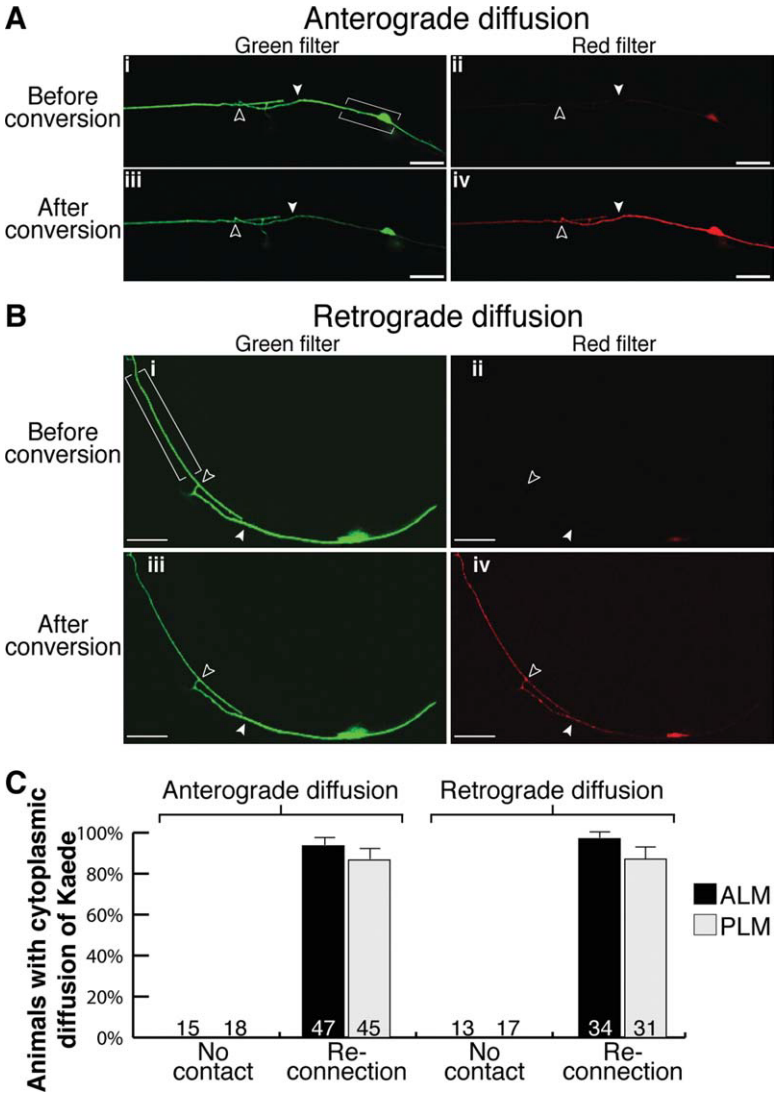

Fig. 3.

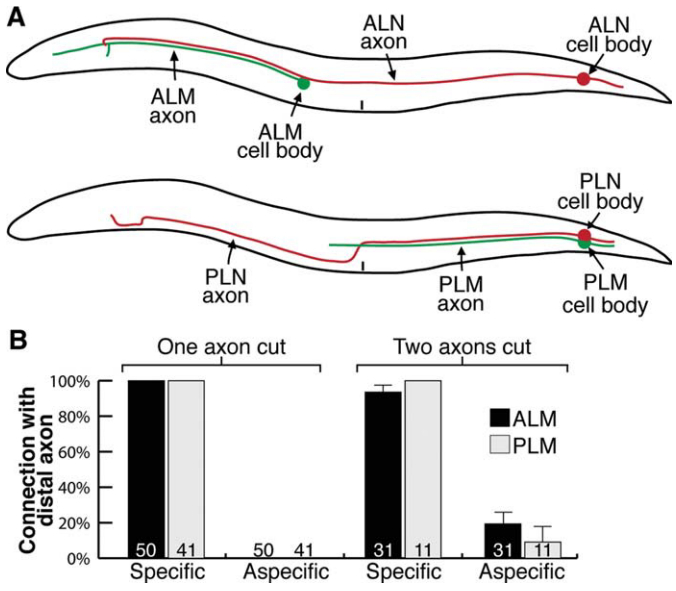

Fig. 4.

When regeneration proceeded without proximal-distal reconnection, converted, red Kaede could not diffuse into the proximal axonal segment (Supp. Fig. S3A,C). However, when reconnection occurred, Kaede converted within the distal axon could diffuse into the proximal axon and cell body (Fig. 3B,C; Supp. Fig. S3D; quantified in Supp. Fig. S3B,E). In every instance of proximal axon regrowth that failed to result in reconnection with the distal fragment, neither anterograde nor retrograde movement of Kaede was observed across the cut site (Fig. 3C). A minor proportion of regrowing axons failed to display anterograde (6% ALM and 13% PLM) or retrograde (3% ALM and 13% PLM) diffusion despite the proximal and distal axon fragments appearing visually reconnected. Interestingly, in these animals the distal axon underwent Wallerian degeneration, indicating that proper axonal fusion had failed, and that it is crucial for efficient axonal regeneration and survival of the distal fragment. Lack of complete axonal fusion is also the

Fig. 3. Axonal fusion re-establishes cytoplasmic continuity. Kaede was converted in PLM in the bracketed regions 24 hr post-axotomy to analyze anterograde (**A**) and retrograde (**B**) cytoplasmic diffusion. Representative images show green and red fluorescence before conversion in panels (i) and (ii), and after conversion in panels (iii) and (iv). Proximal-distal reconnection permitted anterograde (A) and retrograde (B) diffusion of red fluorescent Kaede across the site of axotomy (A, iv; B, iv). Filled arrowheads point to site of axotomy; open arrowheads show fusion site; scale bars = 25 μm. **C**: Quantification of animals displaying either anterograde or retrograde diffusion of Kaede in the absence (no contact) or presence of reconnection for both ALM and PLM. Error bars: standard error of proportion; n values within each graph. Note the presence of a weak background signal before conversion through the red filter (A, B).

Fig. 4. Specificity in axonal fusion. **A**: Schematic diagrams of the *zdIs5(Pmec-4::GFP); vdEx166(Plad-2::mCherry)* strain where ALM and PLM were visualized with green fluorescence and ALN and PLN with red fluorescence. **B**: Quantification of the number of axons displaying specific or aspecific fusion following axotomy of either ALM or PLM (left bars, one axon cut), or after simultaneous axotomy of both ALM and ALN, or PLM and PLN (right bars, two axons cut). Error bars: standard error of proportion; n values within each graph.

most plausible explanation for the distal fragment degeneration found in a minority of GFP-expressing neurons in which reconnection was observed (compare Figs. 1F and 3C). Taken together, these results conclusively demonstrate that axonal regeneration occurs by way of axonal fusion, with re-establishment of both membrane and cytoplasmic continuity.

We next asked whether axonal fusion displayed specificity, whereby regenerating axons could selectively find their own separated fragments. To analyze this, we generated a transgenic strain in which we could visualize sets of two axons running in close association but labeled with two different fluorophores. The ALN and PLN neurons are each bilateral, with cell bodies in the lumbar ganglion and a long process that extends almost the entire length of the animal, terminating within the nerve ring (White, 1986). The ALN and ALM neurites fasciculate for much of the length of ALM, whereas PLN and PLM fasciculate for approximately three quarters of the length of the PLM axon (White, 1986). TEM analysis of serial sections confirmed fasciculation of PLM and PLN at the site of axotomy (Supp. Fig. S4). We expressed mCherry from the *lad-2* promoter (*Plad-2::mCherry*) to visualize PLN and ALN, while ALM and PLM were visualized as previously described with GFP (*Pmec-4::GFP*) (Fig. 4A). We first asked whether a regrowing axon could fuse non-specifically to an intact, second axon. We performed axotomy of ALM and PLM and analysed the ALN and PLN neurons for the presence of GFP. Diffusion of the GFP into the mCherry-expressing neuron would imply that an aspecific fusion event had occurred. GFP was never observed in ALN nor PLN (Fig. 4B), indicating that when a single axon is severed, the regenerating process can specifically fuse with its own distal fragment. We then asked whether a regrowing axon could maintain its ability to specifically fuse with its own distal fragment even when in the presence of a second severed axon of another neuron. To achieve this, we performed paired axotomies on ALM and ALN, as well as PLM and PLN, and 24 hr post-axotomy analyzed each pair of neurons for the transfer of fluorophores. We found a high rate of specificity for both ALM (94%) and PLM (100%) (Fig. 4B). However, a small number of aspecific fusion events, occurring concurrently with specific fusion, were observed in both ALM and PLM (ALM 4/31; PLM 1/11); complete aspecific fusion (not associated with specific fusion) was never found in PLM, and only two cases were observed in ALM. Interestingly, we observed that both ALN and PLN axons displayed a high propensity for regeneration and that they also presented specific proximal-distal reconnection (Supp. Fig. S5). Overall, axonal fusion displayed specificity in almost every instance for both ALM and PLM, even when an adjacent axon was simultaneously severed. These findings may suggest the existence of signaling and cross-talk between the distal fragment and its regrowing axon to ensure specific reconnection and fusion occur.

DISCUSSION

We demonstrate here that axonal fusion with restoration of membrane and cytoplasmic continuity is a key mechanism of axonal regeneration in *C. elegans* neurons. We observe that axonal fusion is necessary to re-establish the original axonal tract, and to prevent degeneration of the separated distal fragment that otherwise invariably occurs in a Wallerian fashion. Our results support and extend to a genetically amenable organism previous observations in different invertebrate species where axonal fusion has been described as an important mechanism underlying successful axonal regeneration after injury (Hoy et al., 1967; Birse and Bittner, 1976; Deriemer et al., 1983). An interesting prediction for the fusion model is that the regrowing axon must be able to find its own separated fragment in order to reform the correct axonal shaft. Our experiments indeed show that the regrowing proximal axons of both ALM and PLM neurons can specifically recognize their own separated distal fragments, even in the presence of a second distal fragment of another severed neuron. These results strongly suggest that specific signaling events regulate self-recognition between separated fragments of the same axon to ensure accuracy. Compared to traditional models of axonal regeneration, axonal fusion represents a fundamentally different mechanism by which restoration of the original axonal tract can be achieved. This modality appears highly efficient for the re-establishment of connection with target tissue, in that transected axons can restore their trajectories by bridging just the damage site instead of regrowing their entire length beyond an injury site. Membrane fusion has been described and extensively studied in important biological events such as endocytosis, exocytosis, plasma membrane sealing, mitochondrial fusion, and viral infection, and several molecules have been identified in each of these processes (Harrison, 2008; Martens and McMahon, 2008; Rizo and Rosenmund, 2008). It would seem likely that some of the molecules regulating membrane fusion in these biological processes are also key elements in axonal fusion during regeneration.

The nematode-specific fusogen Epithelial Fusion Failure 1 (EFF-1) has been reported to be required for axonal reconnection (Ghosh-Roy et al., 2010). However, disruption of the *eff-1* gene led to a significant reduction in regrowth after axotomy and its role in mediating specific axonal fusion is still unclear. EFF-1 functions in homotypic fusion of epithelial and muscle cells (Mohler et al., 2002), and has recently been shown to regulate dendritic pruning in the *C. elegans* PVD neuron (Oren-Suissa et al., 2010). EFF-1, along with the other nematode-specific fusion molecule AFF-1 (Anchor cell Fusion Failure) (Sapir et al., 2007), appears to play an essential role in most, if not all, cellular fusion events in *C. elegans*. The finding of axonal fusion events in different species (Hoy et al., 1967; Birse and Bittner, 1976; Deriemer et al., 1983) may imply that conserved molecules are required for the process to occur, and the discovery of these molecular players will be critical for furthering our understanding of this regenerative mechanism.

It is tempting to speculate on the existence of a "save-me" signaling pathway to mediate recognition between the dying distal fragment and the regrowing proximal axon segment.

Such a signaling mechanism could be reminiscent of the "eat-me" signaling pathway that occurs during the process of apoptotic cell recognition by phagocytic cells. This signaling pathway begins with the presentation of phosphatidylserine on the surface of the dying cell (Fadok et al., 1992), which is then either directly or indirectly recognized by several different classes of receptors on the phagocytic cell surface (Erwig and Henson, 2008; Fadeel and Xue, 2009). Furthermore, it has become apparent that secreted molecules, such as the nucleotides ATP and UTP (Elliott et al., 2009) and the transthyretin-like protein, TTR-52 (Wang et al., 2010), are integral components of this recognition process. However, an alternative and equally plausible hypothesis is that the unique local extracellular environment of the axon mediates specificity of axonal fusion by giving it easier access to its own separated fragments. Moreover, intrinsic neuronal differences, for example, type of neurotransmitter used (ALM and PLM use glutamate, while ALN and PLN use acetylcholine), may also have a role in ensuring fusion occurs specifically. Whether specific molecules, such as those involved in phagocytosis, or whether other factors unique to individual neurons mediate self-recognition during axonal fusion remains to be determined.

Peripheral and central nerve injuries cause significant life-long disabilities because repair rarely leads to reinnervation of the target tissue. Our results suggest that similar mechanisms might be in place, or could be exploited, to enhance axonal regeneration and repair in higher mammals including humans and provide mechanistic insight and support for the development of therapeutic strategies for nerve injuries based on facilitating axonal membrane sealing and reconnection.

EXPERIMENTAL PROCEDURES

Strains and Genetics

Standard techniques were used for *C. elegans* maintenance, crosses, and other genetic manipulations (Brenner, 1974). All experiments were performed at 22°C. The wild-type N2 Bristol isolate, and the following transgenes were used: *zdIs5*[*Pmec-4::GFP*], *vdEx128*[*Pmec-4::Kaede* (10 ng/μl)], *vdEx166*[*Plad-2::mCherry* (25 ng/μl), *Podr-1::dsRED* (30 ng/μl)]. The *zdIs5* strain was kindly provided by Scott Clark.

Molecular Biology

Standard molecular biology techniques were used. The *Pmec-4::Kaede* plasmid was generated through modification of the *Pmec-4::GFP* plasmid in which the GFP coding sequence was excised with KpnI/EcoRI and replaced with the full Kaede coding sequence (amplified from plasmid pMH22, containing *Pdyf-7::Kaede*) (Heiman and Shaham, 2009). The *Plad-2::mCherry* plasmid was created through insertion of a 5.25-kb FseI/AscI fragment of the *lad-2* 5′UTR (amplified using the following primers: external forward 5′-aatttaccttggtcctc ggg-3′; external reverse 5′-tagtgcgaagt accttcaacc-3′; internal forward 5′-tcagt gggccggccagcgaattgcccacttttggcaacc-3′; internal reverse 5′-tcagtgggcgcgcctgttg gaaaaatccaaaaaaaaaagtctgc-3′) and a KpnI/EcoRI mCherry amplicon into the pSM vector (a gift from Cori Bargmann).

Laser Axotomy and Microscopy

Animals were anaesthetized on agar pads using 0.01–0.05% Tetramisole. We performed laser axotomy using a MicroPoint Laser System Basic Unit attached to a Zeiss Axio Imager A1 (Objective EC Plan-Neofluar 100×/1.30 Oil M27). This laser delivers 120 μJoules of 337 nm energy with a 2–6-nsec pulse length. Axotomies were completed with 20 to 30 pulses on larval stage-4 animals at a point approximately 50 μm anterior to the ALM, PLM, and PLN cell bodies, and approximately 500 μm from the cell body of ALN. Animals were analyzed with a Zeiss Axio Imager Z1 equipped with a Photometrics Cool Snap HQ^2 camera and analysis was performed using Metamorph software. Axon regrowth was quantified by measuring the length of the longest ALM or PLM process beyond the cut site 24 hr post-axotomy; neurons that underwent axonal fusion were excluded from these quantifications.

Conversion of Kaede

Kaede experiments were performed with a LSM 510 META confocal microscope and Zen 2008 software. Green fluorescence was analyzed with a 488-nm laser and red fluorescence was visualized with a 543-nm laser. Conversion was achieved with 100 iterations of 405-nm irradiation (1% transmission at 30 mW) to a region of interest (created around the cell body and a short section of the attached processes for analysis of anterograde diffusion; around the distal axon anterior to the cut or fusion site for retrograde studies; or around the entire ALM neuron, except for the nerve ring branch, for analysis of diffusion across gap junctions). For maximum conversion, 20 to 30 repetitions across the region of interest were needed, requiring a total of 5–10 min on average. Exposure to 488-nm light did not cause green-red conversion of Kaede, as analyzed by prolonged exposure (10 min) to this wavelength and subsequent analysis of fluorescence intensity (data not shown). Diffusion of Kaede, either before or after axotomy, has never been observed across the gap junctions formed between the mechanosensory neurons and their contacting neurons (as judged by complete lack of fluorescent signal in these neurons).

Changes in fluorescence intensity were calculated using ImageJ software. Mean fluorescence was measured in the middle of each axon with a line scan on the proximal axonal end immediately adjacent to the transection site and on the distal axon end adjacent to the site of axotomy or fusion. Identically sized regions were used for each group of images. Ratios were calculated between mean fluorescence after conversion and mean fluorescence before conversion, and these were calculated for both green and red fluorescence. As such, a value of 1.0 indicated no change had occurred, a value greater than 1.0 indicated an enhancement of fluorescence in the region of interest, and a value lower than 1.0 indicated reduced fluorescence.

Electron Microscopy

Twenty-four hours post-axotomy of PLM, fluorescence imaging of animals was used to compare cell anatomy prior to fixation. Single animals were fixed

in buffered aldehydes, then in osmium tetroxide, en bloc stained with uranyl acetate, and positioned in groups in agar cubes prior to embedment in Epon resin (Hall, 1995). Serial thin sections were collected onto plastic-coated slot grids (Pioloform) from multiple animals at once, and post-stained with uranyl acetate. Digital TEM images were collected using iTEM software on an Olympus Morada camera mounted on a Philips CM10 electron microscope. Sites of damage and repair were located due to their proximity to the rectal valve cells; this consistent locale helped to re-locate damage sites efficiently within several thousand serial sections.

Statistical Analysis

Statistical analyses were performed using Primer of Biostatistics 3.01. Error of proportions was used to assess variation across a single population. Two-way comparison was performed using the Student's *t*-test.

ACKNOWLEDGMENTS

We thank Casey Linton for assistance in preparation of the *vdEx166* strain; Chris Crocker for help in EM figures preparation; Max Heiman and Shai Shaham for the Kaede coding sequence; Scott Clark for the *zdIs5* strain; Jane Ellis for assistance in TEM preparation; Luke Hammond for support with confocal microscopy; Max Heiman, Rowan Tweedale, Kang Shen, Paolo Bazzicalupo, and Cori Bargmann for critical discussions and reading of the manuscript; Elia di Schiavi, Sean Coakley, Leonie Kirszenblat, Divya Pattabiraman, Nick Valmas, and other members of the Hilliard lab for helpful discussions and comments. Nematode strains used in this work were provided by the *Caenorhabditis* Genetics Center, which is funded by the NIH National Center for Research Resources (NCRR), and the International *C. elegans* Gene Knockout Consortium. This work was supported in part by grant NIH R01-NS060129 (A.B-Y, M.A.H., D.H.H.) and NHMRC Project Grants 631634 and 569500 (M.A.H.).

REFERENCES

Ando R, Hama H, Yamamoto-Hino M, Mizuno H, Miyawaki A. 2002. An optical marker based on the UV-induced green-to-red photoconversion of a fluorescent protein. Proc Natl Acad Sci USA 99:12651–12656.

Benson MD, Romero MI, Lush ME, Lu QR, Henkemeyer M, Parada LF. 2005. Ephrin-B3 is a myelin-based inhibitor of neurite outgrowth. Proc Natl Acad Sci USA 102:10694–10699.

Birse SC, Bittner GD. 1976. Regeneration of giant axons in earthworms. Brain Res 113:575–581.

Bounoutas A, Chalfie M. 2007. Touch sensitivity in *Caenorhabditis elegans*. Pflugers Arch 454:691–702.

Brenner S. 1974. The genetics of *Caenorhabditis elegans*. Genetics 77:71–94.

Deriemer SA, Elliott EJ, Macagno ER, Muller KJ. 1983. Morphological evidence that regenerating axons can fuse with severed axon segments. Brain Res 272:157–161.

Elliott MR, Chekeni FB, Trampont PC, Lazarowski ER, Kadl A, Walk SF, Park D, Woodson RI, Ostankovich M, Sharma P, Lysiak JJ, Harden TK, Leitinger N, Ravichandran KS. 2009. Nucleotides released by apoptotic cells act as a find-me signal to promote phagocytic clearance. Nature 461: 282–286.

Erwig LP, Henson PM. 2008. Clearance of apoptotic cells by phagocytes. Cell Death Differ 15:243–250.

Fadeel B, Xue D. 2009. The ins and outs of phospholipid asymmetry in the plasma membrane: roles in health and disease. Crit Rev Biochem Mol Biol 44: 264–277.

Fadok VA, Voelker DR, Campbell PA, Cohen JJ, Bratton DL, Henson PM. 1992. Exposure of phosphatidylserine on the surface of apoptotic lymphocytes triggers specific recognition and removal by macrophages. J Immunol 148: 2207–2216.

Gabel CV, Antonie F, Chuang CF, Samuel AD, Chang C. 2008. Distinct cellular and molecular mechanisms mediate initial axon development and adult-stage axon regeneration in *C. elegans*. Development 135:1129–1136.

Ghosh-Roy A, Chisholm AD. 2010. *Caenorhabditis elegans*: a new model organism for studies of axon regeneration. Dev Dyn 239:1460–1464.

Ghosh-Roy A, Wu Z, Goncharov A, Jin Y, Chisholm AD. 2010. Calcium and cyclic AMP promote axonal regeneration in *Caenorhabditis elegans* and require DLK-1 kinase. J Neurosci 30: 3175–3183.

Hall DH. 1995. Electron microscopy and three-dimensional image reconstruction. Methods Cell Biol 48:395–436.

Hammarlund M, Nix P, Hauth L, Jorgensen EM, Bastiani M. 2009. Axon regeneration requires a conserved MAP kinase pathway. Science 323:802–806.

Harel NY, Strittmatter SM. 2006. Can regenerating axons recapitulate developmental guidance during recovery from spinal cord injury? Nat Rev Neurosci 7: 603–616.

Harrison SC. 2008. Viral membrane fusion. Nat Struct Mol Biol 15:690–698.

Heiman MG, Shaham S. 2009. DEX-1 and DYF-7 establish sensory dendrite length by anchoring dendritic tips during cell migration. Cell 137: 344–355.

Hilliard MA. 2009. Axonal degeneration and regeneration: a mechanistic tug-of-war. J Neurochem 108:23–32.

Hoy RR, Bittner GD, Kennedy D. 1967. Regeneration in crustacean motoneurons: evidence for axonal fusion. Science 156:251–252.

Loewenstein WR. 1981. Junctional intercellular communication: the cell-to-cell membrane channel. Physiol Rev 61: 829–913.

Low K, Culbertson M, Bradke F, Tessier-Lavigne M, Tuszynski MH. 2008. Netrin-1 is a novel myelin-associated inhibitor to axon growth. J Neurosci 28: 1099–1108.

Macagno ER, Muller KJ, DeRiemer SA. 1985. Regeneration of axons and synaptic connections by touch sensory neurons in the leech central nervous system. J Neurosci 5:2510–2521.

Martens S, McMahon HT. 2008. Mechanisms of membrane fusion: disparate players and common principles. Nat Rev Mol Cell Biol 9:543–556.

Mohler WA, Shemer G, del Campo JJ, Valansi C, Opoku-Serebuoh E, Scranton V, Assaf N, White JG, Podbilewicz B. 2002. The type I membrane protein EFF-1 is essential for developmental cell fusion. Dev Cell 2:355–362.

Moore DL, Blackmore MG, Hu Y, Kaestner KH, Bixby JL, Lemmon VP, Goldberg JL. 2009. KLF family members regulate intrinsic axon regeneration ability. Science 326:298–301.

Neumann S, Bradke F, Tessier-Lavigne M, Basbaum AI. 2002. Regeneration of sensory axons within the injured spinal cord induced by intraganglionic cAMP elevation. Neuron 34:885–893.

Neumann S, Woolf CJ. 1999. Regeneration of dorsal column fibers into and beyond the lesion site following adult spinal cord injury. Neuron 23: 83–91.

Oren-Suissa M, Hall DH, Treinin M, Shemer G, Podbilewicz B. 2010. The fusogen EFF-1 controls sculpting of mechanosensory dendrites. Science 328: 1285–1288.

Pasterkamp RJ, Anderson PN, Verhaagen J. 2001. Peripheral nerve injury fails to induce growth of lesioned ascending dorsal column axons into spinal cord scar tissue expressing the axon repellent Semaphorin3A. Eur J Neurosci 13: 457–471.

Rizo J, Rosenmund C. 2008. Synaptic vesicle fusion. Nat Struct Mol Biol 15: 665–674.

Sapir A, Choi J, Leikina E, Avinoam O, Valansi C, Chernomordik LV, Newman AP, Podbilewicz B. 2007. AFF-1, a FOS-1-regulated fusogen, mediates fusion of the anchor cell in *C. elegans*. Dev Cell 12:683–698.

Simpson I, Rose B, Loewenstein WR. 1977. Size limit of molecules permeating the junctional membrane channels. Science 195:294–296.

Spira ME, Oren R, Dormann A, Ilouz N, Lev S. 2001. Calcium, protease activation, and cytoskeleton remodeling underlie growth cone formation and neuronal regeneration. Cell Mol Neurobiol 21:591–604.

Wang X, Li W, Zhao D, Liu B, Shi Y, Chen B, Yang H, Guo P, Geng X, Shang Z, Peden E, Kage-Nakadai E, Mitani S, Xue D. 2010. *Caenorhabditis elegans* transthyretin-like protein TTR-52 mediates recognition of apoptotic cells by the CED-1 phagocyte receptor. Nat Cell Biol 12: 655–664.

White JG. 1986. The structure of the nervous system of the nematode *C. elegans*. Phil Trans R Soc Lond B Biol Sci 314:1–340.

Wu Z, Ghosh-Roy A, Yanik MF, Zhang JZ, Jin Y, Chisholm AD. 2007. *Caenorhabditis elegans* neuronal regeneration is influenced by life stage, ephrin signaling, and synaptic branching. Proc Natl Acad Sci USA 104: 15132–15137.

Yanik MF, Cinar H, Cinar HN, Chisholm A, Jin Y, Yakar AB. 2006. Nerve regeneration in *C. elegans* after femtosecond laser axotomy. IEEE J Select Top Quant ELectr 12:1283–1291.

Yanik MF, Cinar H, Cinar HN, Chisholm AD, Jin Y, Ben-Yakar A. 2004. Neurosurgery: functional regeneration after laser axotomy. Nature 432:822.

Yiu G, He Z. 2006. Glial inhibition of CNS axon regeneration. Nat Rev Neurosci 7:617–627.

Figure S1. Kaede cannot pass across gap junctions. Two gap junctions are formed in the nerve ring between the ALM and AVM neurons. (**A**) Prior to conversion of Kaede, ALM and AVM (cell bodies and axons) are visible in the green channel with only a weak signal in the ALM cell body through the red channel. (**B**) Kaede was converted throughout the entire ALM axon, except for the nerve ring branch, leading to a strong increase in red fluorescence and decrease in green signal due to conversion of the protein from its green form to its red form. The converted red form of the protein could not pass from the ALM axon into the AVM axon. Arrowhead points towards the end of the ALM nerve ring branch, where the red form of Kaede could diffuse no further. It should also be noted that green fluorescent Kaede or GFP has never been observed to pass through the gap junctions formed by ALM (with PVR), AVM (with AVD), PLM (with PVC, LUA, PVR, PHC) or PVM (with AVL and PDE). Images in each panel represent projection of three different planes. Scale bars: 25 µm.

Figure S2. Analysis of anterograde diffusion and quantification of changes in fluorescence intensity. Kaede was converted in the bracketed region in PLM 4 hrs (**A**), or in ALM 8 hrs (**C**) or 24 hrs (**D**) post-axotomy to analyze anterograde cytoplasmic diffusion. Representative images for green and red fluorescence before conversion are shown in panels (i) and (ii), and after conversion in panels (iii) and (iv). Without proximal-distal reconnection (**A**,**C**), red fluorescence was absent from the distal segment (**A**,iv; **C**,iv). Upon reconnection (**D**) red fluorescence was evident within the distal segment (**D**,iv). Changes in fluorescence intensity following conversion of Kaede were quantified for both PLM (**B**) and ALM (**E**). A line scan was performed on the proximal

and distal axon segments before and after conversion, and a ratio created between the two values to provide an indication of the changes in green and red fluorescence. Animals presenting no axonal reconnection displayed decreased green and increased red fluorescence following conversion in the proximal axon and no change in the distal axon, as cytoplasmic continuity had been disrupted. After proximal-distal reconnection, a reduction in green and an enhancement of red fluorescence occurred in both the proximal and distal axon segments, indicating that cytoplasmic continuity had been re-established. The ratio of red fluorescence provides a quantification of the movement of the converted protein across the fusion site. Error bars represent standard error of the mean; n values for no reconnection and fusion in (**B**) are 38 and 42 animals, respectively and in (**E**) 29 and 46 animals, respectively; scale bars: 25 µm; * $p < 0.05$; ** $p < 0.0001$ compared to no reconnection.

Figure S3. Analysis of retrograde diffusion and quantification of changes in fluorescence intensity. Kaede was converted in the bracketed region in PLM (**A**), or in ALM (**C**,**D**) 24 hrs post-axotomy to analyze retrograde cytoplasmic diffusion. Shown are green and red fluorescence images before conversion in panels (i) and (ii), and after conversion in panels (iii) and (iv). Without proximal-distal reconnection (**A**,**C**), red fluorescence was absent from the proximal segment (**A**,iv; **C**,iv). Upon reconnection (**D**) red fluorescence was evident within the proximal segment and cell body (**D**,iv). Changes in fluorescence intensity following conversion of Kaede were quantified for both PLM (**B**) and ALM (**E**). A line scan was performed on the proximal and distal axon segments before and after conversion, and a ratio created between the two values to provide an

indication of the changes in green and red fluorescence. Animals presenting regrowth without reconnection between proximal and distal axon segments displayed decreased green and increased red fluorescence following conversion in the distal axon and no change in the proximal axon as cytoplasmic continuity had been disrupted. After axonal fusion, a reduction in green and an enhancement of red fluorescence occurred in both the distal and proximal axon segments due to the re-establishment of cytoplasmic diffusion. Error bars represent standard error of the mean; n values for no reconnection and fusion in (**B**) are 17 and 27 animals, respectively and in (**E**) are 13 and 32 animals, respectively; scale bars: 25 µm; * $p < 0.001$; ** $p < 0.0001$ compared to no reconnection.

Figure S4. Association between PLM and PLN. Electron microscopy shows the regrowing side branches of PLM grow inward away from the cuticle and damage zone. Top six panels show selected electron micrographs where PLM (green) and PLN (yellow) are traced in the serial thin sections (section numbers marked on top left corner of each panel). The proximal process of PLM lies close to the cuticle, at the bottom of each panel, and a branch extends inward from it in sections #1516-1518. Note that the new branch also sends off a shorter side branch to the upper left which stops, whereas the small green process in the upper right of #1518 can be followed around the laser damage zone towards the distal fragment of the original PLM axon (data not shown). The PLM side branch also encloses a small mitochondrion at its base (sections #1516-1517). The sections in the bottom four panels were tilted in the electron microscope to better display the microtubule bundles of PLN (yellow). Within these sections, PLN is seen to extend a new inward branch in section #1514, but the complete connection to the inward growing

portion of PLN was never captured. The upper yellow profile in section #1515 travels around the laser damage zone to the distal fragment of the original PLN process (data not shown). The microtubules inside PLN are all of similar, normal diameter, while those inside PLM are a mixture of two sizes, including some enlarged, as is characteristic only for the mechanosensory neurons. White arrows in panels #1516 and #1517 indicate a slight swelling of the extracellular space where mantle protein is secreted by PLM, another characteristic of the mechanosensory neurons. Scale bar: 100 nm.

Figure S5. Analysis of ALN and PLN regeneration following axotomy. Quantification of the regenerative characteristics of the ALN and PLN axons 24 hrs post-axotomy. Regrowth is defined as sprouting from proximal end, distal contact represents the proportion of regrowing neurons that made contact with their distal fragment, and distal maintenance illustrates the percentage of reconnecting neurons that preserved the distal axon segment. Error bars represent standard error of proportion; n values are 61 and 32 for ALN and PLN, respectively.

Figure S1

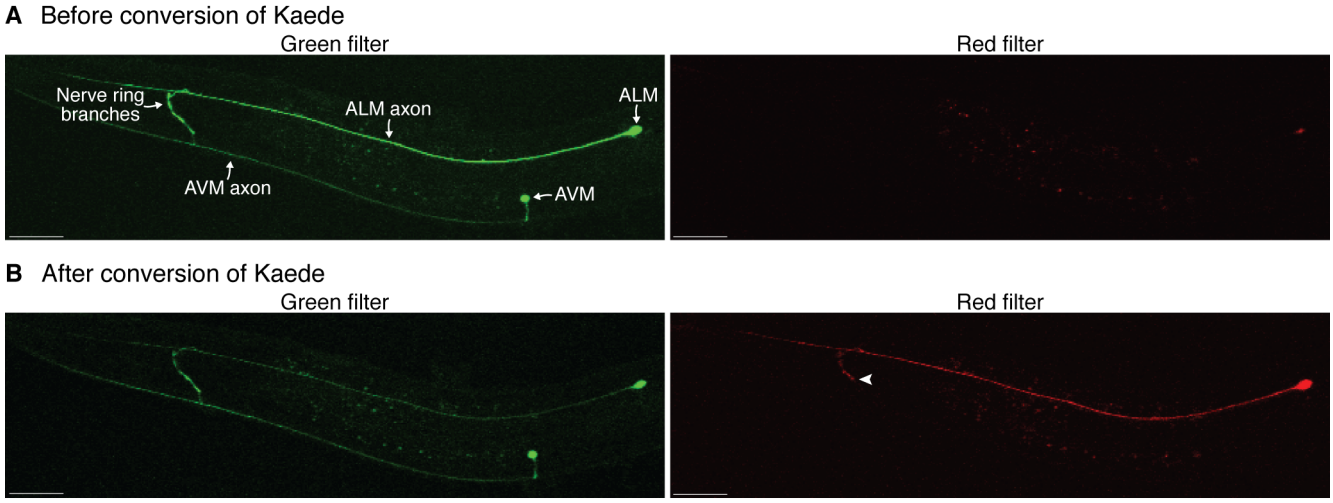
A Before conversion of Kaede
Green filter
Red filter
Nerve ring branches
ALM axon
ALM
AVM axon
AVM
B After conversion of Kaede
Green filter
Red filter

Figure S2

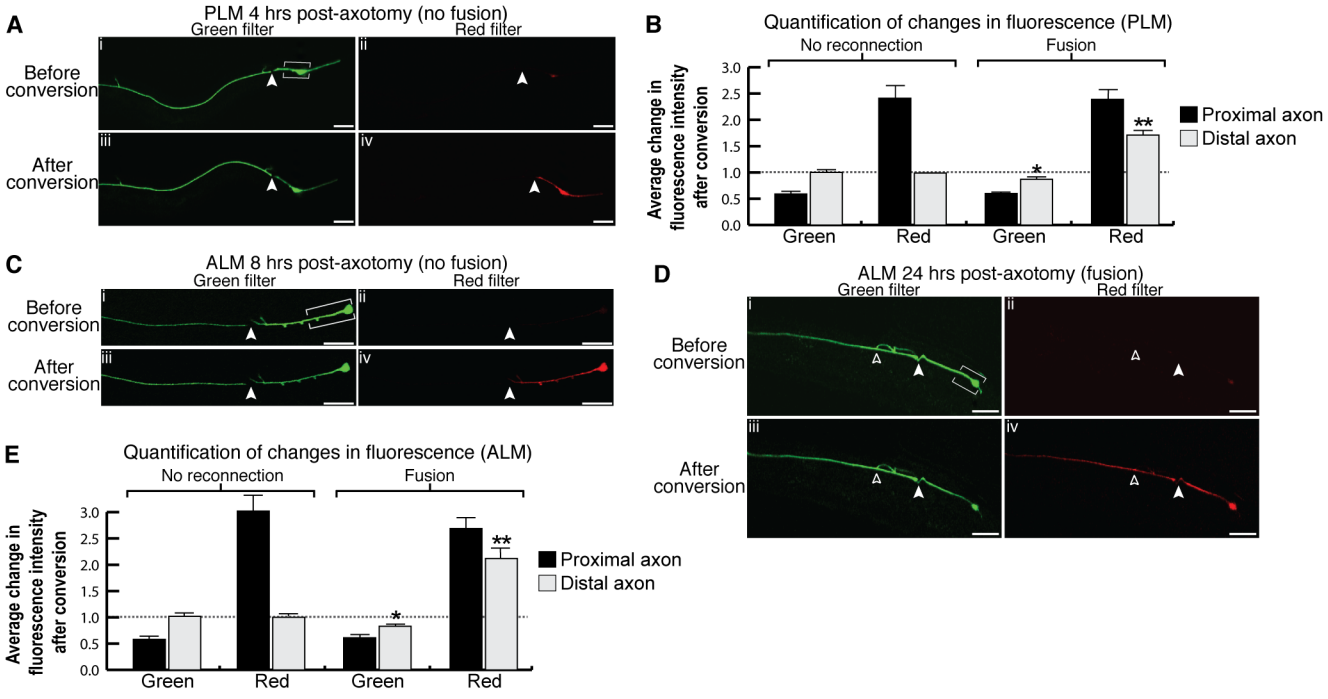
A
PLM 4 hrs post-axotomy (no fusion)
Green filter
Red filter
Before conversion
After conversion
i
ii
iii
iv
B
Quantification of changes in fluorescence (PLM)
No reconnection
Fusion
Average change in fluorescence intensity after conversion
3.0
2.5
2.0
1.5
1.0
0.5
0.0
Green
Red
Green
Red
**
*
Proximal axon
Distal axon
C
ALM 8 hrs post-axotomy (no fusion)
Green filter
Red filter
Before conversion
After conversion
i
ii
iii
iv
D
ALM 24 hrs post-axotomy (fusion)
Green filter
Red filter
Before conversion
After conversion
i
ii
iii
iv
E
Quantification of changes in fluorescence (ALM)
No reconnection
Fusion
Average change in fluorescence intensity after conversion
3.0
2.5
2.0
1.5
1.0
0.5
0.0
Green
Red
Green
Red
**
*
Proximal axon
Distal axon

Figure S3

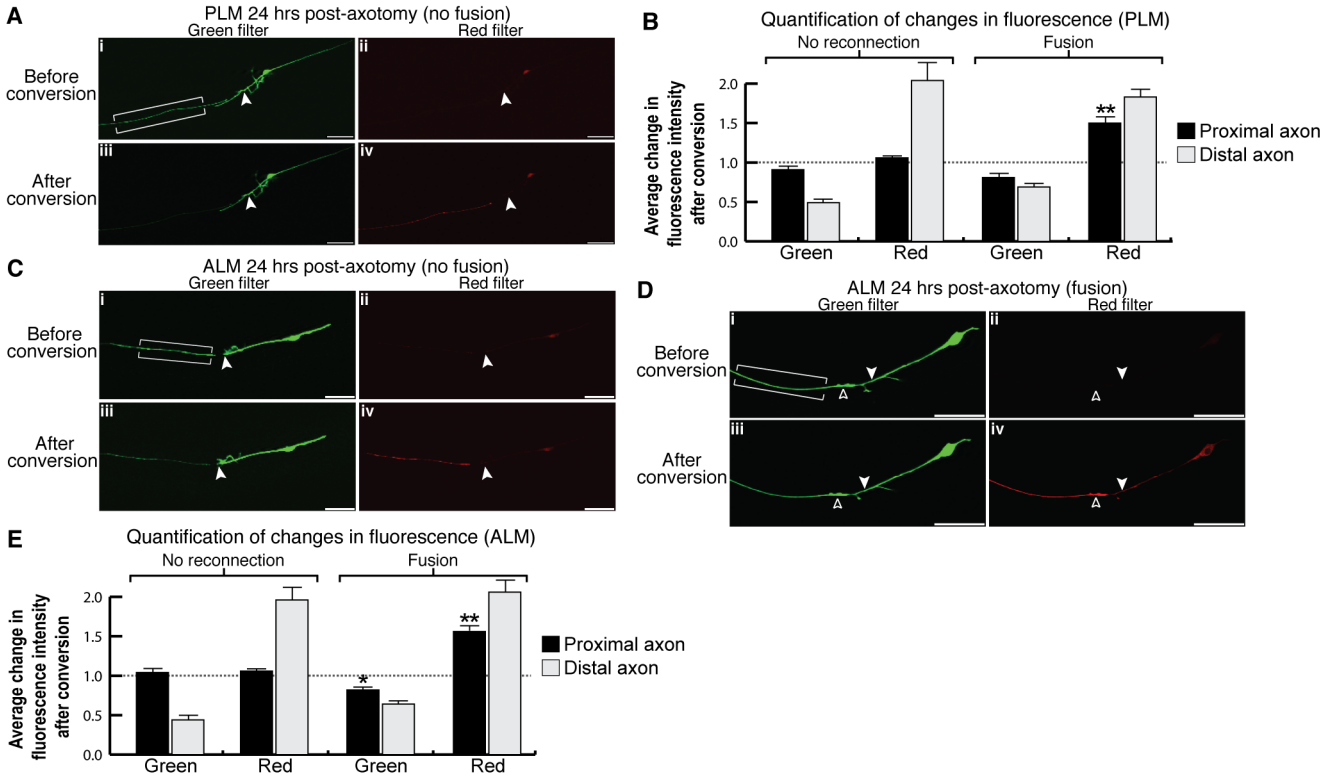
A
PLM 24 hrs post-axotomy (no fusion)
Green filter
Red filter
Before conversion
After conversion
i
ii
iii
iv
B
Quantification of changes in fluorescence (PLM)
No reconnection
Fusion
Average change in fluorescence intensity after conversion
2.0
1.5
1.0
0.5
0.0
**
Green
Red
Green
Red
Proximal axon
Distal axon
C
ALM 24 hrs post-axotomy (no fusion)
Green filter
Red filter
Before conversion
After conversion
i
ii
iii
iv
D
ALM 24 hrs post-axotomy (fusion)
Green filter
Red filter
Before conversion
After conversion
i
ii
iii
iv
E
Quantification of changes in fluorescence (ALM)
No reconnection
Fusion
Average change in fluorescence intensity after conversion
2.0
1.5
1.0
0.5
0.0
*
**
Green
Red
Green
Red
Proximal axon
Distal axon

Figure S4

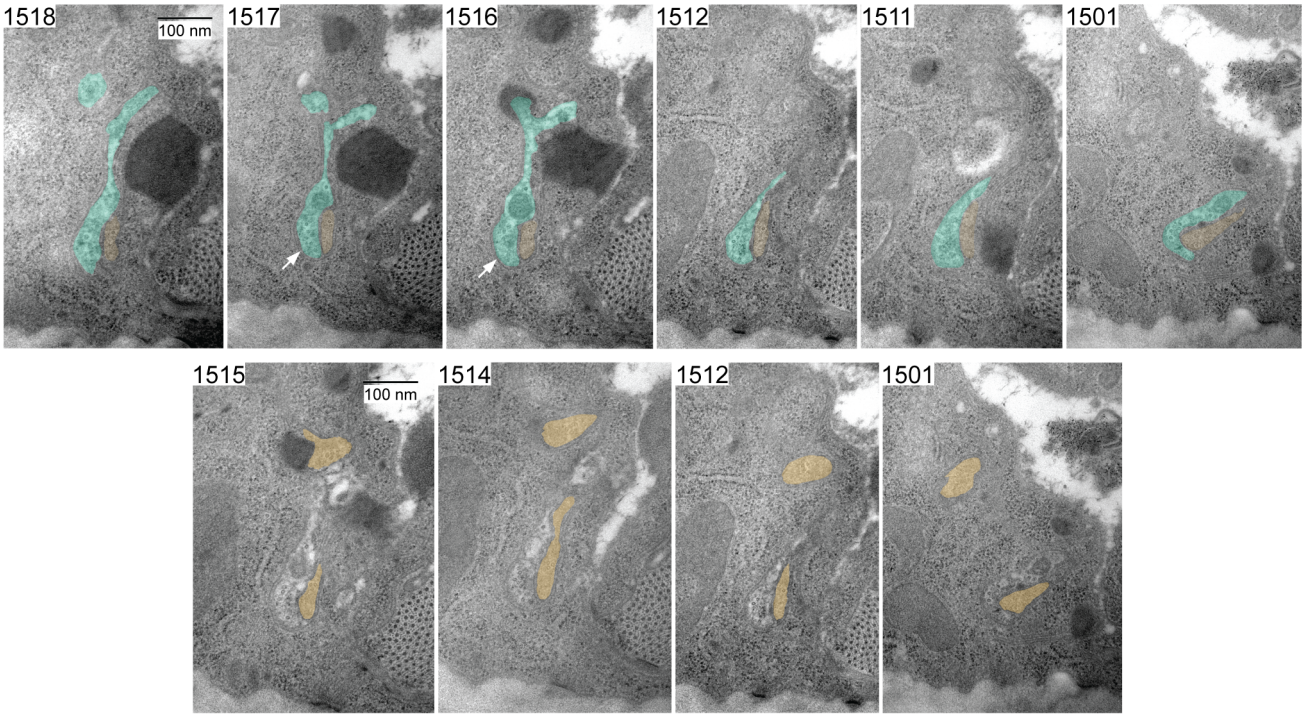
1518
100 nm
1517
1516
1512
1511
1501
1515
100 nm
1514
1512
1501

Figure S5

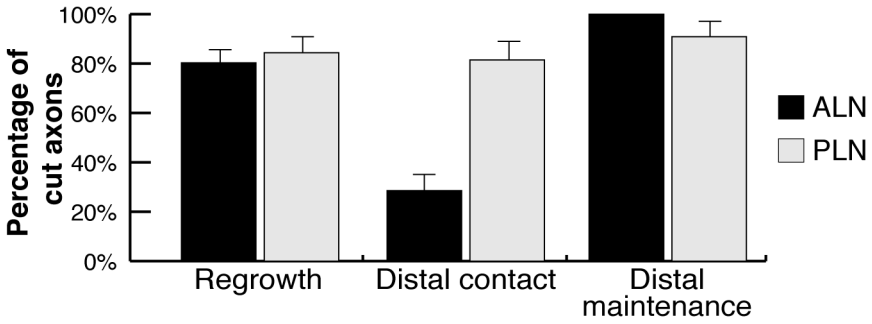
Percentage of cut axons
100%
80%
60%
40%
20%
0%
Regrowth
Distal contact
Distal maintenance
ALN
PLN